

ration value  $-(\mu - \mu_g)n$  and  $\chi = 0$ . We see once again the jumps occurring at  $p'H/n = 1, \frac{1}{2}, \frac{1}{3}, \dots$ . This behavior is shown in Fig. 2.

An interesting feature in this case is the possibility that  $\chi$  changes sign at each magnetization jump,

$$\begin{aligned} \chi &= 2(s+1)p'\mu_g \quad (s \text{ odd}), \\ &= -2sp'\mu_g \quad (s \text{ even}). \end{aligned} \quad (6)$$

The explanation for this peculiar transition is, in fact, very simple. As the diamagnetic property is dominated by the  $k=1$  Landau level, the change in  $M$  is to be determined by the spin levels. If the separation between  $l=1$  and  $l=2$  levels,  $3\epsilon_0$ , is larger than  $2\mu_g H$ , there is no crossing between different spin levels. When  $s$  is even, there are equal numbers of  $\sigma=+1$  and  $\sigma=-1$  filled levels each containing  $pH$  electrons.  $\chi$  is determined by the  $(s+1)$ th partially filled  $\sigma=-1$  state. A decrease in  $H$  will increase the net number of polarized moments in the  $\sigma=-1$  state, and  $M$  will thereby increase; hence  $\chi$  is negative. When  $s$  is odd, the uppermost filled state is  $\sigma=-1$  and the remaining electrons reside on the  $(s+1)$ th partially filled  $\sigma=+1$  state. A decrease in  $H$  will increase the number of electrons in this  $\sigma=+1$  state and reduce the net magnetization, and hence  $\chi$  is positive.

The above simple picture breaks down when  $3\epsilon_0$  becomes smaller than  $2\mu_g H$ ; the  $l=1, \sigma=+1$  state now lies above the  $l=2, \sigma=-1$  level. When this level crossing takes place, the energy scheme

becomes a little more complicated, but we have an enhancement in the polarized electrons. When  $3\epsilon_0 < 2\mu_g H$ , complete polarization can be achieved at  $\frac{1}{2}H_0$  instead of  $H_0$ .

The conditions for case (A),  $\epsilon_0 > \mu H > \mu_g H$ , can be fulfilled in films of simple metals with  $d \sim 20 \text{ \AA}$ ,  $H \sim 100 \text{ kG}$  ( $\epsilon_0 \sim 10^{-13} \text{ erg}$ ,  $\mu H \geq 10^{-15} \text{ erg}$ ) and in films of semimetals such as Bi with  $d \sim 100 \text{ \AA}$ ,  $H \sim 70 \text{ kG}$  ( $\epsilon_0 \sim 10^{-13} \text{ erg}$ ,  $\mu H \sim 10^{-14} \text{ erg}$ ). To achieve  $\mu H > \mu_g H$ , we need to find an orientation in which the cyclotron mass is smaller than the spin effective mass, e.g., the trigonal axis direction in Bi.

To satisfy the conditions for case (B),  $\mu H > \epsilon_0 > \mu_g H$ , in simple metals seems impossible. The short electron wavelength in these metals ( $\sim 20 \text{ \AA}$ ) makes  $\epsilon_0$  very large. The magnetic field required to achieve  $\mu H \sim \epsilon_0$  is around  $10^7 \text{ G}$ , far beyond our present capability. However, the semimetals Bi and its dilute alloys (e.g., Bi-Sb, Bi-Te) with  $d \sim 300 \text{ \AA}$ ,  $H \sim 200 \text{ kG}$ , will correspond to  $\mu H \geq 3 \times 10^{-14} \text{ erg}$ ,  $\epsilon_0 \leq 10^{14} \text{ erg}$ , and  $\mu_g H \sim 6 \times 10^{-15} \text{ erg}$ , and thus we may find transitions corresponding to case (B) in films of these materials.

<sup>1</sup>For a recent review, see, for example, V. B. Sandmirskii, Zh. Eksp. Teor. Fiz. 52, 158 (1967) [Sov. Phys. JETP 25, 101 (1967)].

<sup>2</sup>L. E. Gurevich and A. Ya. Shik, Zh. Eksp. Teor. Fiz. 54, 1873 (1968) [Sov. Phys. JETP 27, 1006 (1968)].

<sup>3</sup>The expressions for case (A) have first been given by Gurevich and Shik in Ref. 2.

## Comparison of $p$ - $p$ and $n$ - $p$ Quasi-free Scattering in $p + d \rightarrow p + p + n$ Reaction

V. Valkovic,\* D. Rendic,\* V. A. Otte, and G. C. Phillips

*T. W. Bonner Nuclear Laboratories, † Rice University, Houston, Texas 77001*

(Received 21 December 1970)

Proton-proton and proton-neutron quasielastic scattering-process contributions were measured simultaneously at a proton energy of 12 MeV with  $\theta_{1p} = -30^\circ$ ,  $\theta_{2p} = \theta_n = 30^\circ$ . The ratio of the peak cross sections  $(\sigma_{np}/\sigma_{pp})_{\text{exp}}$  was found to be  $2.0 \pm 0.2$ , while the simple impulse approximation predicts  $(\sigma_{np}/\sigma_{pp})_{\text{imp}} = 1.3$ . No Coulomb effects were found to be significant.

Recently the study of proton-neutron quasi-free scattering (QFS) in the  ${}^2\text{H}(p, pn)p$  reaction was reported by Petersen *et al.*<sup>1</sup> In comparison with the kinematically equivalent  ${}^2\text{H}(p, pp)n$  reaction<sup>2,3</sup> it was found that the measured cross section for  $(p, pn)$  QFS was a factor of 3 to 4 larger than that of  $(p, pp)$  QFS at bombarding energies below 20 MeV. In Refs. 1 and 3, application of the impulse

approximation failed to explain this difference in magnitude, although the theoretical results could be normalized to fit the peak shape. It was suggested<sup>3</sup> that the effect may be caused by the Coulomb force.

The proton-proton QFS experiment in Refs. 2 and 3 was performed by detection of two protons at  $43^\circ$  on opposite sides of the beam direction in

the scattering plane, while in the  ${}^2\text{H}(p, pn)p$  experiment<sup>1</sup> the proton and neutron were detected at  $45^\circ$  on opposite sides of the beam. The proton-neutron QFS peak shape agrees with a normalized impulse-approximation calculation, while in the  $(p, pp)$  reaction it was noted that the observed spectra were narrower than those calculated.<sup>2,4</sup>

In order to study the reported differences in  $p$ - $p$  and  $p$ - $n$  QFS in the  $p+d \rightarrow p+p+n$  reaction, an experiment with the simultaneous detection of  $p$ - $p$  and  $p$ - $n$  coincidences were performed. The 12-MeV proton beam from the Rice University tandem Van de Graaff accelerator was used to bombard a deuterated polyethylene target. The two outgoing protons from the  $p+d \rightarrow p+p+n$  reaction were detected using surface-barrier silicon detectors at  $\theta_1 = -\theta_2 = 30^\circ$  with respect to beam axis. Simultaneously the proton-neutron coincidences were detected at  $\theta_1 = -\theta_n = 30^\circ$  using liquid-scintillator neutron detectors. The details of the experimental arrangement will be published<sup>5</sup> separately. The angular settings for all the detectors were chosen to achieve maximum separation of QFS and final-state-interaction (FSI) contributions. Careful attention was paid to the determination of the neutron-counter efficiency, which was determined using the  $d+d \rightarrow n+{}^3\text{He}$  reaction. Outgoing  ${}^3\text{He}$  particles were detected by a surface-barrier,  $\Delta E/\Delta x-E$  counter telescope. The neutron-detector efficiency was obtained as the ratio of the (simultaneously determined) number of detected  ${}^3\text{He}$  particles in coincidence with associated neutrons and the number of  ${}^3\text{He}$  particles without that requirement. Measured neutron-proton coincidence spectra were corrected for the experimentally-determined neutron-counter efficiency.

Three independent measurements of  $p$ - $p$  and  $p$ - $n$  coincidences from  $p+d \rightarrow p+p+n$  reaction were performed. The spectra obtained are shown in Fig. 1 as a projection on the common proton-energy axis. The experimental peak cross section for  $p$ - $p$  QFS is  $5.8 \pm 0.5$  mb/sr<sup>2</sup> MeV, while for  $n$ - $p$  QFS it is  $11.7 \pm 0.5$  mb/sr<sup>2</sup> MeV. The ratio of observed  $n$ - $p$  and  $p$ - $p$  QFS contributions is much smaller than that reported in Ref. 1. Both experimental spectra, when normalized, have the same shape and are symmetrical around the minimum spectator-particle energy. This fact indicates that the effect of Coulomb forces is negligible since otherwise the  $p$ - $p$  and  $p$ - $n$  coincidence spectra would be shifted with respect to each other.

In Fig. 1 the solid line represents the impulse-

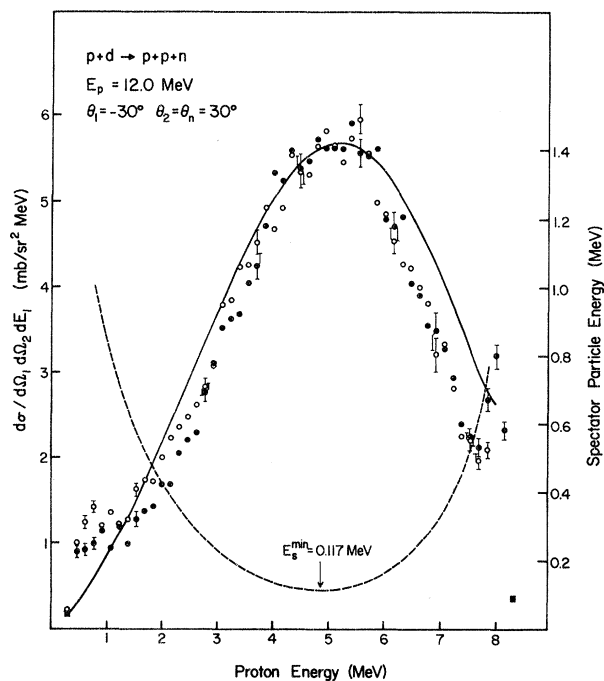


FIG. 1. Proton-proton (solid dots) and proton-neutron (open circles) coincidence spectra projected on common proton-energy axis. Neutron-proton spectrum is normalized by  $N=0.5$ . Solid line is impulse-approximation prediction normalized to  $p$ - $p$  experimental data by  $F=0.2$ . Dashed line is spectator-particle laboratory energy.

approximation calculation<sup>6</sup> normalized to the proton-proton coincidence spectra with  $F=0.2$ . The impulse approximation predicts that the ratio of  $n$ - $p$  and  $p$ - $p$  QFS cross sections for 12 MeV and  $\theta_1 = -\theta_2 = 30^\circ$  is  $(\sigma_{np}/\sigma_{pp})_{imp} = 38.97/29.89 = 1.3$ . The experimentally determined value is  $(\sigma_{np}/\sigma_{pp})_{exp} = 2.0 \pm 0.2$ . The similarity of  $p$ - $p$  and  $p$ - $n$  spectral shapes indicates that they differ by a multiplicative factor, since the difference due to an additive term would produce shapes of the normalized spectra which would be expected to be different. Such a multiplicative factor might be obtained by taking into account  $p$ - $p$  and  $n$ - $p$  FSI contributions in the region of the QFS peaks. In the case of  $p$ - $p$  QFS only the  $n$ - $p$  FSI can contribute to the cross section (each proton interacting with a spectator neutron). In the case of  $n$ - $p$  QFS both  $n$ - $p$  and  $p$ - $p$  FSI can contribute to the cross section since the unobserved particle is a proton. In the region of the QFS peaks final-state interactions for rather large relative energies have to be taken into account. The  $p$ - $p$  FSI extends to higher relative energies than the  $n$ - $p$  FSI thus making the observable  $n$ - $p$  QFS cross section larger than the  $p$ - $p$  QFS. Numerical calculation

along these lines are in progress.

In conclusion it can be said that the mechanism of the  $p+d \rightarrow p+p+n$  reaction is fairly well understood by considering only QFS along with FSI processes.

The authors would like to thank Dr. W. von Witsch, Dr. M. Ivanovich, and Dr. W. E. Sweeney for their help in the various stages of the experiment.

\*On leave from Institut "Ruder Boskovic," Zagreb,

Yugoslavia.

†Work supported in part by the U. S. Atomic Energy Commission.

<sup>1</sup>E. L. Petersen *et al.*, Phys. Lett. **31B**, 209 (1970).

<sup>2</sup>W. J. Braithwaite *et al.*, in *Three Body Problem*, edited by J. S. McKee and P. M. Ralph (North-Holland, Amsterdam, 1970), p. 407.

<sup>3</sup>D. J. Margaziotis *et al.*, Phys. Rev. C **2**, 2050 (1970).

<sup>4</sup>I. Slaus *et al.*, Phys. Lett. **23**, 358 (1966).

<sup>5</sup>V. Valkovic, D. Rendic, V. A. Otte, W. von Witsch, and G. C. Phillips, to be published.

<sup>6</sup>A. F. Kuckes, R. Wilson, and P. F. Cooper, Ann. Phys. (New York) **15**, 193 (1961).

## Spins and Parities of Highly Excited States in $Mg^{24}$ †

A. Gobbi, P. R. Maurenzig,\* L. Chua, R. Hadsell, P. D. Parker, M. W. Sachs, D. Shapira, R. Stokstad, R. Wieland, and D. A. Bromley

A. W. Wright Nuclear Structure Laboratory, Yale University, New Haven, Connecticut 06520

(Received 21 December 1970)

From a study of the reaction  $C^{12}(O^{16}, \alpha_1)Mg^{24}(\alpha_2)Ne^{20}$ , spins and parities have been measured for states in  $Mg^{24}$  at the following excitation energies (in MeV): 12.10 ( $4^+$ ), 12.45 ( $7^-$ ), 13.07 ( $5^-$ ), 14.41 ( $4^+$ ), 16.07 ( $6^+$ ), and 16.59 ( $6^+$ ). Branching ratios were measured for several states in  $Mg^{24}$  with  $13 \leq E_{exc} \leq 23$  MeV decaying to the following states in  $Ne^{20}$ :  $0^+$  (ground state),  $2^+$  (1.63 MeV), and  $4^+$  (4.25 MeV). These results permit the elimination of several postulated structures for the states in question.

The recent observation<sup>1</sup> of several unexpected narrow-width states in  $Mg^{24}$  at excitation energies near 16 MeV which are strongly populated in the reaction  $O^{16}(C^{12}, \alpha)Mg^{24}$  suggests a number of interesting and different possibilities for the structure of levels in this energy region. It is presently a matter of conjecture whether these are high-spin members of rotational bands, quasimolecular states,<sup>2</sup>  $\alpha$  clusters,<sup>3</sup> or, possibly, structures of some other type. Spin and parity assignments are obviously of fundamental importance in the determination both of their nature and of the reaction mechanisms whereby they are populated. In this Letter we report new experimental information on the spins, parities, and branching ratios for a number of states in  $Mg^{24}$  in the region of excitation  $12 \leq E_{exc} \leq 23$  MeV, obtained from a study of the reaction  $C^{12}(O^{16}, \alpha_1)Mg^{24}(\alpha_2)Ne^{20}$  at  $E_{O^{16}} = 48.0, 48.8, \text{ and } 58.3$  MeV (lab).

States above 9.32 MeV in  $Mg^{24}$  are unbound to  $\alpha$  decay. A measurement of the angular correlation of their decays to the  $0^+$  ground state of  $Ne^{20}$  enables a straightforward determination of the spin and parity  $J^\pi$  of the parent states in  $Mg^{24}$ . Since the ground-state spins and parities of  $O^{16}$ ,  $C^{12}$ , and  $He^4$  are all  $0^+$ , and since  $\alpha_1$  is detected

along the beam axis, only normal-parity states are observed<sup>4</sup> and the angular correlation of  $\alpha_2$  leading to the  $Ne^{20}$  ground state is proportional to  $P_J^2$ , where  $P_J(\cos\theta)$  is the Legendre polynomial of order  $J$ . A 10-mm  $\times$  50-mm position-sensitive, solid-state detector (PSD) subtending laboratory angles from  $25^\circ$  to  $90^\circ$  recorded all particles with  $E_{lab} \geq 2$  MeV which were in coincidence with  $\alpha$  particles emerging in a  $10^{-2}$ -sr solid angle at  $0^\circ$ . Silver and nickel absorber foils sufficiently thick ( $\sim 20$  mg/cm<sup>2</sup> in total) to stop the incident  $O^{16}$  beam were placed between the 20- $\mu$ g/cm<sup>2</sup> carbon target and the  $dE/dx$ - $E$  solid-state counter telescope at  $0^\circ$ . For each coincident event,  $E_{\alpha_1}$ ,  $E_{\alpha_2}$ ,  $P_{\alpha_2}$ , and  $T_{\alpha_1-\alpha_2}$  were recorded on magnetic tape, where  $E$ ,  $P$ , and  $T$  denote energy, position, and time. These data were analyzed and sorted on the basis of the reaction kinematics in a multiparameter space both on and off line with the laboratory's IBM 360/44 data acquisition system. The absolute position calibration of the PSD was obtained with a precision of  $\pm 1^\circ$  in a separate measurement in which a grid was placed over the face of the detector. Figure 1 shows an example of a two-dimensional display of selected coincident events obtained at 48.0 MeV for the transition to the  $Ne^{20}$